Experimental Investigation of Flow Distortion in Fan-in-Wing Inlets

U. W. SCHAUB*
National Research Council of Canada, Ottawa, Canada

Extending earlier investigations, the aerodynamic performance of a datum inlet with circular arc lips was evaluated. The lip radius-to-diameter ratio was 0.09, and tests were conducted both with and without a set of radial and annular vanes. Other inlets assessed included one with sharp-edged lips, and another with an elliptic leading lip (major axis perpendicular to the wing chord line). The "mixed vane" configuration in the datum inlet reduced the extent of separated flow in the inflow ratio range 0.0 to 0.7. It was also especially effective in attenuating the residual momentum over the entire range. The sharp-edged inlet data were helpful primarily in comparing the present results with data in hydraulic engineering. Good agreement was exhibited between the velocity distortion index at zero forward speed and the classical flow coefficients for Borda tube entrances. The total pressure loss was qualitatively in concord with Borda tube entrance losses. The elliptic lip inlet extended the unseparated flow regime to inflow ratios 0.45, from 0.25 for the datum inlet.

Nomenclature

D = outer diameter of inlet annulus
p = pressure
q = dynamic pressure = $\frac{1}{2}\rho V^2$
R = inlet lip radius
x,y,z = space coordinates in the directions of chord, span, and inlet axis, respectively
V = velocity
α = wing incidence angle
γ = swirl angle; positive when counter-clockwise as viewed from above the model
δ = inflow misalignment angle = $\tan^{-1}(V_x/V_j)$
Δ = change in a quantity
θ = probe rotation angle; positive when clockwise as viewed from above the model; $\theta = 0°$ in the symmetry plane at the front of the annulus
Q = velocity distortion index, V_j/V_a

Subscripts

a = average based on geometric annulus area
j = average based on active flow area
0 = stagnation condition
s = static condition
∞ = condition in the undisturbed stream

I. Introduction

A PROGRAM of experimental aerodynamic studies involving fan-in-wing inlets has been the subject of two earlier publications. Performance data were offered for a family of three simple inlets and three separate aids intended to improve the inflow at high forward speeds.[1,2] A theoretical method was described and results were given for a two-dimensional potential flow model.[1] For the convenience of the reader, who may not have seen Ref. 1, the pertinent conclusions are restated: 1) inflow distance is the most important variable for achieving a uniform velocity distribution in the inlet, 2) a generous radius ratio inlet produces a less uniform velocity profile than one with a small lip radius-to-diameter ratio, at the same inflow depth, and 3) inlets with small lip radii feature large surface velocity peaks and hence also large diffusion rates.

Presented as Paper 67-746 at the AIAA/RAeS/CASI 10th Anglo-American Aeronautical Conference, Los Angeles, Calif., October 18–20, 1967; submitted December 11, 1967; revision received April 30, 1968.

* Assistant Research Officer, Engine Laboratory, Division of Mechanical Engineering.

The conclusions stated in the previously reported experimental work,[2] although derived from different experimental inlet hardware, are applicable as well to the present work and therefore are recapitulated.

1) There is a general tendency for the inlet-plane flowfield to appear quasi-two-dimensional with velocity magnitudes decreasing in the wing chord direction.

2) The distribution of such flow variables as velocity, total pressure, swirl, and inflow-to-axis angle is a strong function of inlet geometry, degree of flow separation, and wing incidence angle.

3) Maximum local velocity and swirl angle are strongly dependent on inflow ratio and wing incidence. They are of such magnitude that they constitute a serious problem in making the environment of the fan less viable.

4) Leading lip separation, a function of inflow ratio, forward speed, and wall boundary condition, contributes most seriously to the general problem of inflow distortion.

The following work deals with inlet tests completed since the earlier publications. Distortion data are presented for two inflow depth stations in a chosen datum inlet, and for a fixed inflow depth station in three other inlets. Experimental results are discussed in relation to predictions based on the two-dimensional potential flow theory published earlier.

II. Inlet Models

The model comprised a main wing body having a NACA 0015 basic profile. Four inlets were then installed in turn. The wing had a chord length of 80 in. and an aspect ratio of $\frac{3}{2}$. The inlet duct axis was positioned at the 35% chord station and was perpendicular to the plane of the wing. The model was tested in NRC's 10- × 20-ft open-circuit propulsion wind tunnel in the speed range zero to 130 fps. Three wing incidence settings were chosen: −12.5°, 0°, and +12.5°. The tunnel test setup is illustrated schematically in Fig. 1. The inlet air was drawn by plant suction machinery located far away from the model, thereby effectively placing the fan at infinity.

The datum inlet, following previous practice, featured a constant-radius (R/D = 0.09) lip. The second inlet had a square-edged centerbody and outer lip. The third inlet was an asymmetrically shaped trumpet. The fourth inlet comprised an assembly of mixed vanes (both radial and annular segments) in the datum inlet. The last inlet shown in Fig. 2

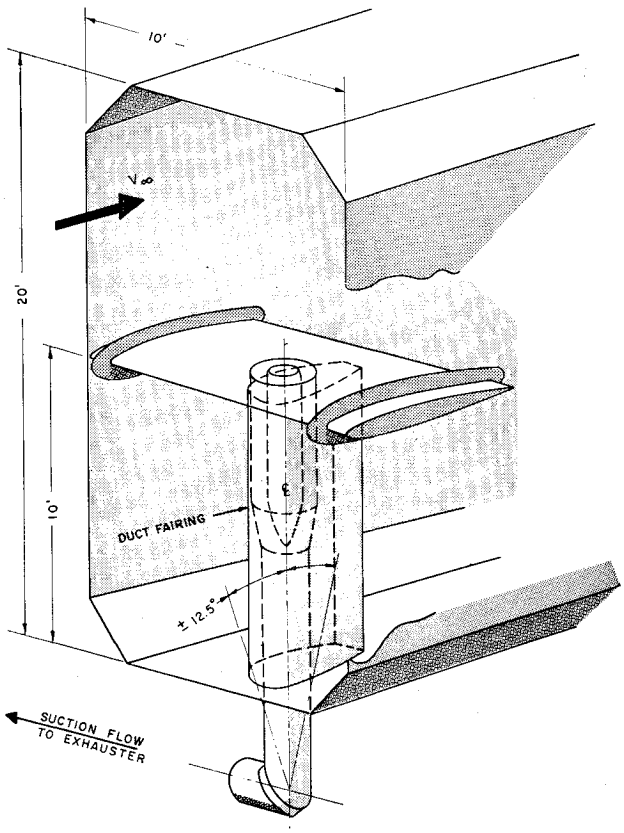

Fig. 1 Installation of the model in the wind tunnel.

was tested earlier and featured a large asymmetrically shaped elliptic lip.

III. Instrumentation

The inflow stream variables were measured with a rake fitted with eight individual probes, each having a probe head comprising a five-tube cluster. Inflow direction, speed, and total pressure at the chosen measuring plane were computed using the three-dimensional calibration characteristics of this probe, applicable for a non-nulling measuring technique.[3]† The measuring plane was normally located on the wing section axis, i.e., at an inflow depth of $D/4$ (station 2), except in the case of the datum inlet where, in addition, measurements were made at a depth of $D/8$ (station 1). The pressure surveys covered the starboard half of the inlet annulus only, lateral flow symmetry having been checked by means of surface pressure taps. The probe was indexed in 15° steps around the semiannulus.

IV. Flowfield Details

Velocity Distributions

The test results in Fig. 3a for $V_\infty/V_a = 0$ taken at station 1 (just below the lower tangent point of the lip) indicate that the velocity profile along any radial line has an "arched" shape with large near-surface velocities at the outer and centerbody walls and smaller ones at midpassage, as shown in Fig. 4.

Large near-surface velocities were predicted for the outer walls by potential flow theory.[1] In an annular inlet the catch flow does not initially sense the presence of the centerbody and accelerates towards the inlet as if it were a simple sink.

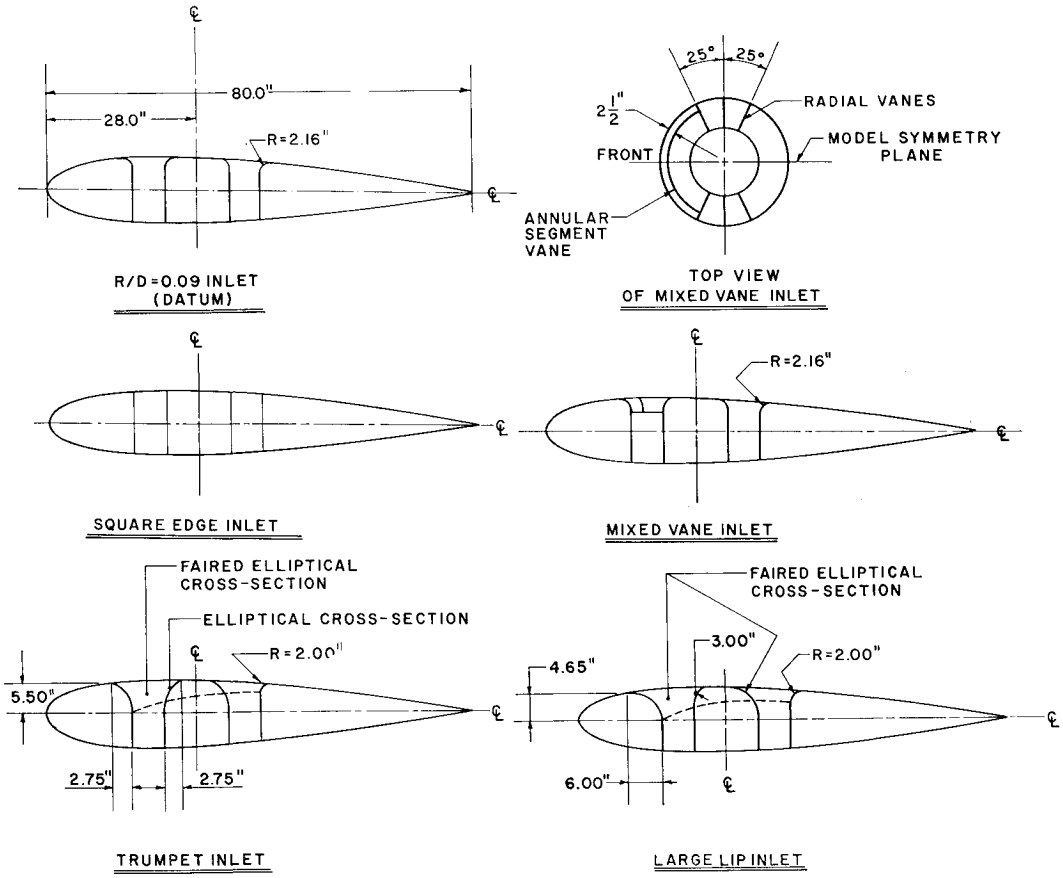

Fig. 2 Wing inlet configurations.

† Although the calibrations permitted velocity vector misalignment cone angles of up to 45° and computations were actually made up to this limit, the measuring uncertainty increased rapidly for cone angles exceeding 35°.

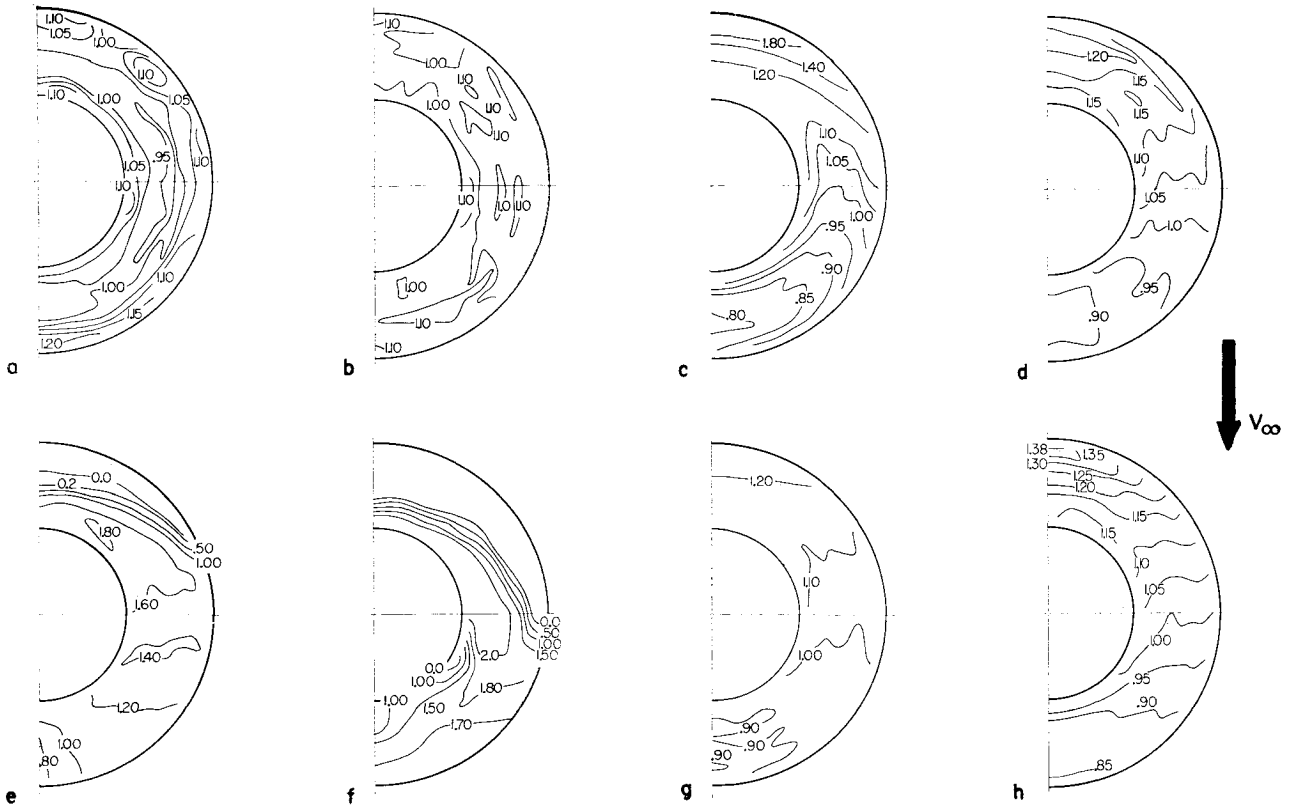

SUB-FIGURE	a	b	c	d	e	f	g	h
INLET MODEL	DATUM	DATUM	DATUM	DATUM	DATUM	SQUARE EDGED	TRUMPET	LARGE LIP
INFLOW RATIO	0.0	0.0	0.30	0.29	0.76	0.78	0.27	0.27
MEASURING DEPTH STATION	D/8	D/4	D/8	D/4	D/4	D/4	D/4	D/4

Fig. 3 Inlet annulus isotachs (V/V_a); wing at zero incidence.

It already has considerable momentum before a further localized secondary acceleration is necessary at the centerbody surface. This causes the near-surface velocities at the centerbody to exceed those in the middle of the passage.

At forward speed the catch flow, having approached unilaterally, must turn 90° as it enters. Although much of the turning takes place externally, it is possible to identify an over-all decrease in the magnitude of velocity in the wing chord direction that is characteristic of flow in a duct bend.

As may be seen from the experimental results, velocity perturbations, a local wall effect, are superimposed on the characteristic velocity field. These perturbations are still discernible at station 1, as shown typically in Fig. 3c.

Inflow distance is a powerful factor in achieving flow uniformity at all forward speeds. This is evidenced by comparing Fig. 3c with 3d, and 3a with 3b. However, near-surface velocity peaks at the inner wall still persist, a phenomenon that may be expected from external aerodynamic considerations. Analogous examples are well known and demonstrate generally that the velocity perturbations near a body require more than a distance of one body diameter to abate.

This basic distribution of velocity has repeatedly been observed in all inlets tested and for all test conditions. In fact, even for adverse test conditions and severe lip geometries, when large flow separations existed, the characteristic profiles were still quite noticeable, as illustrated by Figs. 3e and 3f. Naturally, such inlet flows feature larger isotach levels‡ and a general displacement of isotachs due to the associated flow contractions.

Although the effects of flow bending are predominant in the general velocity profile, lip geometry is also a critically important variable. For one thing, boundary-layer separation takes place partially due to adverse features of surface geometry, and this inflicts major damage on the whole inflow field. For another, although the flow is fully attached, changes in shape of the major suction surface cause second-order modifications to the downstream velocity field. For example, a "large lip" inlet produced a greater velocity nonuniformity than the datum inlet with fully attached flow and at the same inflow depth (compare Figs. 3h and 3d).

Flow Angle Distributions

The two component flow angles, inflow-to-axis and swirl angles, computed from pressure data have distinct significances. The former varies with inlet geometry, inflow distance, and severity of flow separation. For a fan mounted in

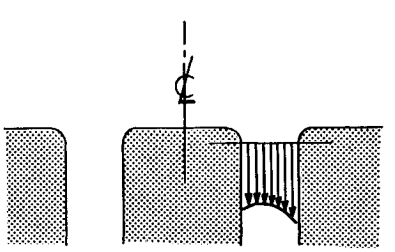

Fig. 4 Schematic velocity profile in the symmetry plane of the model.

‡ Isotachs are defined as lines of constant magnitude of the nondimensional velocity V/V_a.

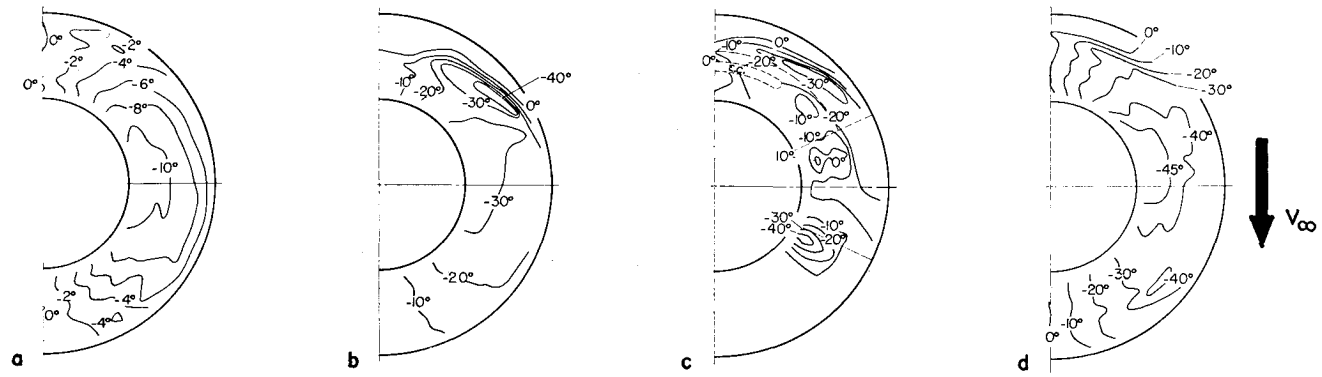

SUB-FIGURE	a	b	c	d
INLET MODEL	DATUM	DATUM	MIXED VANE	DATUM
INFLOW RATIO	0.29	0.76	0.79	0.85
MEASURING DEPTH STATION	D/4	D/4	D/4	D/8

Fig. 5 Swirl angle distributions in the inlet annulus; wing at zero incidence.

a wing, it represents the degree of spanwise flow over its blades and is usually only a second-order effect on fan performance. Swirl angle is of prime significance because it reflects directly on fan blade incidence and tends to be the larger of the two angles away from the symmetry plane. The datum inlet was chosen again to illustrate typically the general distribution of flow direction.

For unseparated inflows at forward speed, maximum swirl tends to be in the annulus sides where the guidance effect of the walls is minimal and, hence, the residual momentum is greatest. Figure 5a illustrates typically for a small inflow ratio of 0.29 that the maximum swirl angle was 10° and that it was located at $\theta = 90°$. When the leading lip can no longer support attached flow, the forward-facing surfaces act on more mass flow than previously, and the maximum swirl region shifts towards the flow separation. The example shown in Fig. 5b illustrates that the maximum swirl was 40° and was centered at $\theta = 50°$. Substantial reduction in swirl angle was achieved by inserting a set of radial vanes, in the sides of the datum inlet (compare Figs. 5c and 5b).

The effect of inflow depth on swirl angle can be assessed by means of Figs. 5d and 5b for the depth stations $D/8$ and $D/4$, respectively. At the former depth station large areas existed

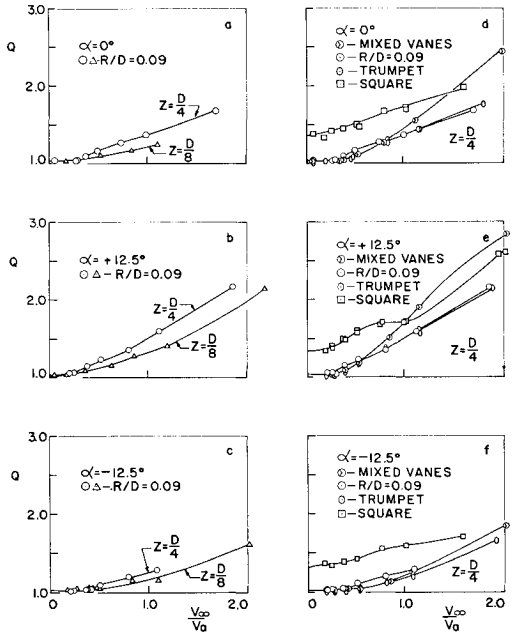

Fig. 6 Velocity distortion index.

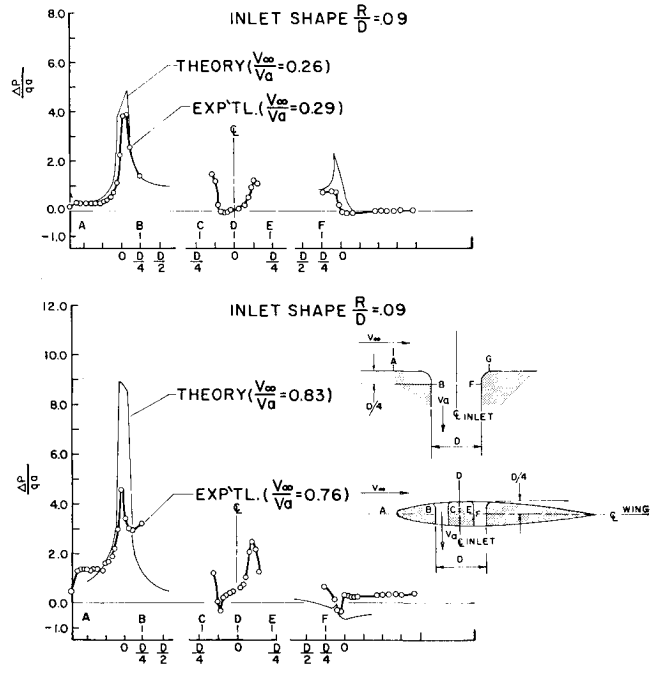

SURFACE DISTANCE (IN ANNULUS DIAMETERS) MEASURED FROM THE D/4 INFLOW DEPTH STATION

Fig. 7 Surface pressure distribution in the symmetry plane of the $R/D = 0.09$ inlet.

with swirl in excess of 45°, whereas at the latter the angles were attenuated by some 10°.

V. Performance Comparisons

Although the distribution plots of the flow variables give detailed information about the flowfield, they are cumbersome to use for comparing the performance of one inlet relative to another over a range of test conditions. The integrated values representing the level of distortion are the same parameters employed previously[2] and, for convenience, are again explained here.

The velocity distortion index (V_j/V_a) is the ratio of the average velocity in the z direction (based on the active flow area) to the design inlet velocity (based on full annulus area). The lowest possible index value is unity. Low index values indicate a low over-all velocity distortion level and one that is generally achieved when the flow is fully attached and boundary layers are thin. Conversely, increasing index ratings signify thickening boundary layers, or a growing separation bubble in the inlet. The velocity distortion index is analogous to the reciprocal of discharge coefficient.

The flow misalignment parameter (δ) is the angle whose tangent is the average x momentum divided by the average z momentum. Since the angle is coplanar with the initial and the final momentum vectors M_∞ and M_z, it is a direct measure of distortion. Axisymmetric inlets ideally feature $\delta = 0°$ at zero forward speed.

The average total pressure loss parameter ($\Delta p_0/q_a$) is useful primarily in traditional assessments of performance, but is not a good measure of distortion. It gives, for instance, inadequate information about the presence, size, and growth of dead flow cavities. Since the regions of fluid shear, which are responsible for the loss, are relatively small compared to the geometric area, the average loss parameter is based on proportionately fewer sampling points. Furthermore, boundary-layer measurements were not made, and only detached flow losses are represented; consequently, the loss data offered suffer from a datum error.§

On the other hand, boundary-layer losses tend to be small in inlets compared to detached shear flow losses so that it is meaningful to use the loss data at least for comparative purposes. Moreover, the loss parameter has a well-established usage as a pressure distortion index for several reasons. For example, it fully accounts for the circumferential variation in total pressure, which has been recognized as being the dominant effect in the deterioration of compressor performance due to distortion at the inlet face.[4] Boundary-layer losses, which are not represented here, influence performance to a lesser extent, particularly for single-stage fans. Also, it is a parameter which in the field of internal aerodynamics has experienced wide usage, especially in matching inlets to compressors.

Velocity Distortion

Generally, the velocity distortion index can be seen to increase with inflow distance (compare the curves labeled $D/8$ and $D/4$ in Fig. 6). Incipience of flow detachment at the leading lip and the rate of dilatation of the resultant separation bubble depend on the inflow ratio. They are promoted also by increasing wing incidence and sharpness of lip.

The velocity distortion index data for the datum inlet are in good qualitative agreement with the surface pressure data

§ If it were assumed that the boundary layer occupied all of the area adjacent to the walls not sampled by the probe (and this would be a pessimistic assumption) approximate calculations would show that the datum error was likely to be between 0.13 and 0.09 dynamic heads. This figure is in fair agreement with the classically recognized entrance loss values of 0.23 to 0.04 dynamic heads for so-called "generously rounded" or "trumpet shaped" inlets, respectively.

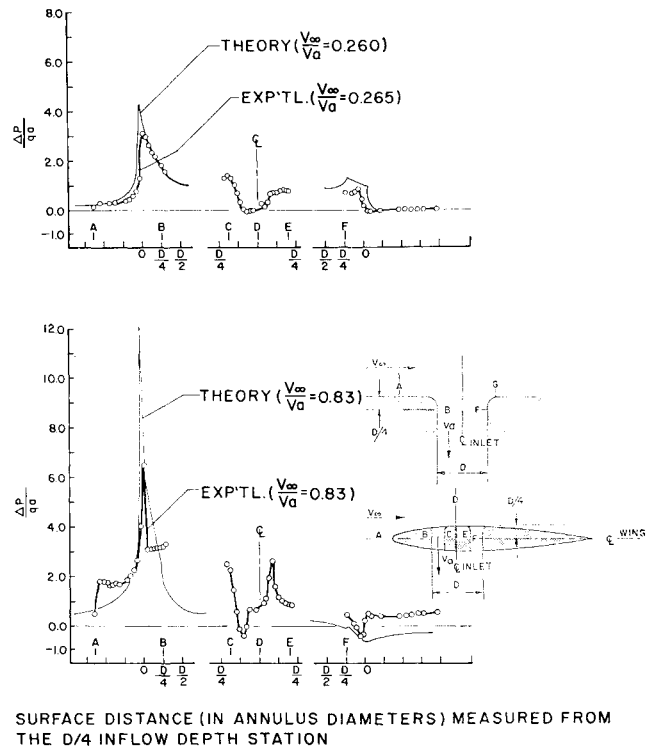

Fig. 8 Surface pressure distribution in the symmetry plane of the trumpet inlet.

illustrated in Fig. 7. These pressure measurements corroborate both the location of the separation boundary on the lip surface and its incipience as a function of inflow ratio.

The square-edged inlet suffered acutely from large-scale flow separation over the entire inflow ratio range. The initial velocity distortion index, shown in Figs. 6d–6f, was $V_j/V_a = 1.32$ and exceeded those values from all other inlets tested. The reciprocal value ($V_a/V_j = 0.76$) compares very well with Borda tube flow coefficients, nominally given as 0.71 if the entrance is followed by several diameters of duct length. The index increased continuously with inflow ratio. For example at the inflow ratio of unity the index for the square-edged inlet was 1.62 whereas for the datum inlet it was only 1.3. At any given inflow ratio and wing incidence setting, the separation problem for the square-edged inlet is well defined and appears to represent a practial limit which other simple inlets may approach, but seldom exceed. It is interesting to observe that the velocity distortion did not change significantly with moderate changes in wing incidence ($-12.5° \leqslant \alpha \leqslant +12.5°$).

The distortion index for the trumpet inlet resembled closely that for the datum inlet, except near the onset of flow separation. For the zero wing incidence case, flow separation was delayed from $V_\infty/V_a = 0.25$ (for the datum inlet) to 0.45. The extended range of attached flow resulted in correspondingly lower distortion index ratings. Obvious differences in surface geometry between the two inlets are thought to bring about the more viable pressure distribution shown in Fig. 8.

The mixed vane configuration was effective in delaying the growth of dead flow at inflow ratios of up to 0.8. At higher inflow ratios still, the vanes failed to retain the dead flow, and the velocity distortion increased eventually more rapidly than in the datum inlet, and eventually faster than in the square-edged inlet.

Flow Misalignment

The trend was towards increased flow misalignment with increasing inflow ratio, as is shown generally in Fig. 9. Initially at zero forward speed the flow misalignment angle should be zero for all except perhaps the asymmetric inlet shapes. Instead, δ was observed to be about 3° to 5°. It is

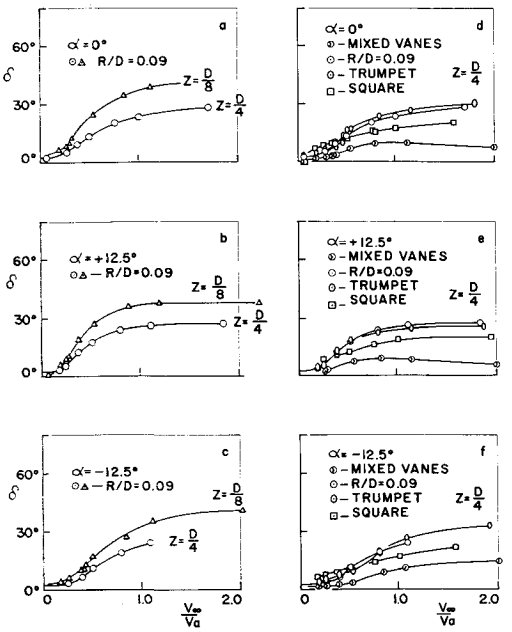

Fig. 9 Misalignment angle parameter.

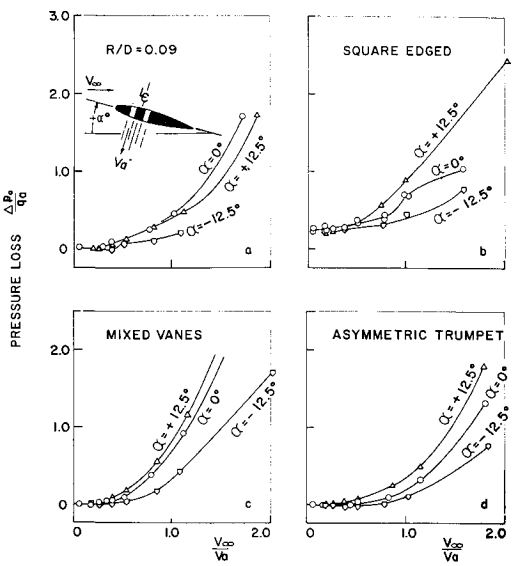

Fig. 10 Total pressure loss.

presumed that this deviation was due to tunnel constraints. Rapid deterioration of the flow alignment was observed to coincide with boundary-layer separation. For unknown reasons the misalignment problem appeared to be self-limiting, depending on both inlet geometry and wing incidence setting. Although it is known that sizable measuring errors at very large inflow ratios ($V_\infty/V_a \geq 1.3$) make exact estimation of limits uncertain, the asymptotic behaviour of the function δ is clearly discernible.

It is useful to recall from potential flow theory that flow uniformity is best achieved by inflow depth and sharpness of bellmouth lip. These predictions were confirmed by experiment for separating as well as for fully attached boundary-layer flow. The influence of inflow depth is well demonstrated by the datum inlet data in Figs. 9a–9c. The effect of sharpness of bellmouth lip is best assessed by comparing the δ curves of the square-edged inlet with those for the datum inlet for badly separated inlet flows at the three wing incidence angles shown in Figs. 9d–9f.

Total Pressure Loss

All inlets featured similar gradual loss increases initially, as shown in Fig. 10. At an inflow ratio of unity the datum inlet, for example, suffered a loss of 0.4 dynamic heads. Negative wing incidence generally diminished losses significantly throughout the entire inflow ratio range.

Extensive flow separation in the square-edged inlet was reflected in the large loss value of 0.24 dynamic heads at zero forward speed. The large dead flow cavity adjacent to the walls insured that a greater percentage of the live flow was sampled by the probe, and hence the datum loss for this inlet was more fully accounted for than for the others. This datum loss does not include the downstream enlargement loss that is normally included in commonly used entrance loss data. If, to a first approximation, the enlargement loss were taken as 0.13 inflow dynamic heads for an enlargement ratio of 1.35,¶ then the cumulative loss would be 0.37 inflow dynamic heads. This value is in concord with Borda tube entrance losses frequently given as 0.34 to 0.43 dynamic heads. Losses built up rapidly with larger inflow ratios and generally were larger for positive wing incidence (see Fig. 10).

¶ This value corresponds to the velocity distortion index value for the square-edged inlet at zero forward speed.

The vane configuration, which was seen to be an effective velocity distortion reducing element, did of course give rise to additional losses due to wakes. Although the lip separation problem at the lower inflow ratios had been reduced, the cumulative losses rapidly exceeded those of the plain $R/D = 0.09$ inlet for inflow ratios greater than 0.5. However, since wing-supported flight would likely be achieved before $V_\infty/V_a = 0.5$, the losses would not be large enough to derogate from the otherwise good serviceability of the mixed vane inlet.

Conclusions

1) Increasing inflow distance reduced inflow velocity profile nonuniformity and misalignment. 2) For any given depth installation small-lipped inlets were preferable to large lipped inlets from a flow distortion point of view, provided that separation could be avoided. 3) It was possible to extend the attached flow regime observed for circular arc lipped inlets through the use of a leading lip contour featuring a radius of curvature that increased with inflow distance. 4) Velocity nonuniformity, the flow misalignment level, and the extent of separated flow were substantially lessened by the insertion of a radial/annular segment vane configuration in the datum inlet; the improvements were accompanied, however, by an associated rise in total pressure loss. 5) Good agreement was exhibited between the measured velocity distortion index at zero forward speed and classical flow coefficients for Borda tube entrances. The total pressure loss was also qualitatively in accord with Borda tube entrance losses.

References

[1] Schaub, U. W. and Cockshutt, E. P., "Analytic and Experimental Studies of Normal Inlets, with Special Reference to Fan-in-Wing VTOL Powerplants," *Proceedings of the International Council of the Aeronautical Sciences*, Spartan, 1965, pp. 519–553.

[2] Schaub, U. W., "Experimental Studies of VTOL Fan-in-Wing Inlets," *Aerodynamics of Power Plant Installation*, AGARDograph 103, Pt. 2, Oct. 1965, AGARD, pp. 715–747.

[3] Schaub, U. W., Sharp, C. R., and Bassett, R. W., "An Investigation of the Three-Dimensional Flow Characteristics of a Non-Nulling Five-Tube Probe," DME Aero. Rept. LR-393, Feb. 1964, National Research Council, Ottawa, Canada.

[4] Dawson, L. G., "The Engine Designer's Point of View," *Aerodynamics of Power Plant Installation*, AGARDograph 103, Pt. 1, Oct. 1965, AGARD, pp. 1–29.